

HOLOGRAPHIC 3-D DISKS

Demetri Psaltis and Allen Pu
California Institute of Technology
Department of Electrical Engineering
Pasadena, California 91125, USA
psaltis, allenpu@sunoetics.caltech.edu

Abstract

The performance characteristics of an experimental holographic 3-D disk system are described. A surface density of 10 bits/ μm^2 is experimentally demonstrated using a 100 μm thick photopolymer as the recording medium.

I. Introduction

Holographic storage was first demonstrated more than 20 years ago^{1,2}. The lack of the necessary optical devices (lasers, spatial light modulators (SLM), detector arrays, deflectors) and recording materials were some of the reasons why holographic storage did not become practical at that time. In addition, there was not an urgent need for the capabilities afforded by holographic storage. The situation has now changed completely. The dramatic advances in electronic computers have led to ever increasing demand for inexpensive mass storage devices. Optical storage devices have emerged as the preferred technology for removable ROM media. It does not appear, however, that the density of conventional 2-D optical storage devices (e.g. CD-ROM) will be able to increase rapidly enough to satisfy the requirements of some applications. Therefore, a 3-D memory technology, such as holographic storage, is now very much in demand. During the last decade, optoelectronic technology has provided us with a rich variety of compact, inexpensive, and high performance semiconductor laser diodes, liquid crystal SLMs, and CCD detector arrays. The recent resurgence of interest in holographic storage has taken place largely because we have been able to use these modern components to perform large scale demonstrations of holographic memories in LiNbO₃^{3,4,5} and photopolymers⁶. In this paper, we will concentrate on a particular holographic memory architecture, the holographic 3-D disk^{7,8}.

The optical setup for storing angle multiplexed holograms is shown in Figure 1. The information to be recorded is presented on the SLM and it modulates the signal beam. The reference beam is a plane wave whose angle of propagation is controlled by a deflector, such as the rotating mirror shown in Figure 1. Multiple holograms are stored by changing the angle of the reference beam while updating the data presented on the SLM. The stored holograms are retrieved by illuminating the hologram with the proper reference beam. The reconstruction is then detected by a CCD camera. Each stored hologram can be independently read-out due to the angular selectivity of thick holograms. For example, if the thickness of the hologram is 1 cm, then the angular selectivity is approximately .005 degrees. Therefore, if the range of angles that can pass through the aperture of the optical system in the reference arm is from -

2.5 to 2.5 degrees, then $M = 5^\circ/0.005^\circ = 1000$ holograms can be angularly multiplexed. The diffraction efficiency of each hologram is⁹:

$$\eta = \left(\frac{M/\#}{M} \right)^2 \quad (1)$$

where $M/\#$ is a constant depending on the parameters of the recording medium and the optical setup. A typical value for a 1 cm thick LiNbO₃ crystal is $M/\# \sim 5$, which yields a diffraction efficiency in excess of 10^{-5} when 1,000 holograms are stored. With this diffraction efficiency, a laser with output power on the order of tens of mW is sufficient to read out the reconstructed holograms at video rate, using conventional CCDs. We have also stored 10,000 angularly multiplexed holograms at a single location in LiNbO₃ using a sufficiently thick crystal¹⁰. However, the accompanying loss in diffraction efficiency (by a factor of 100 according to Equation (1)) would make it very difficult to realize a practical system with 10,000 superimposed holograms unless the $M/\#$ can be sufficiently increased.

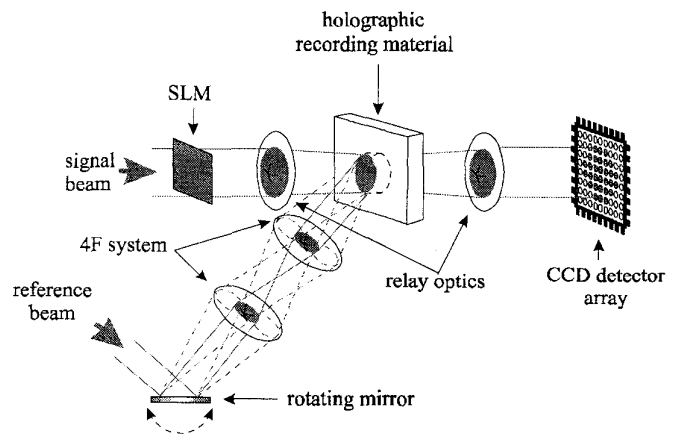


Figure 1 : Angle Multiplexing setup.

The storage capacity of a holographic memory of the type shown in Figure 1 is equal to the number of holograms multiplexed, M , multiplied by the number of bits per stored page. If the SLM used to record the holograms has 1000×1000 pixels and $M = 1000$, then the storage capacity is 1 gigabit. Since optical disks currently have capacity more than a gigabyte, it is clear that a simple holographic memory would not be competitive in terms of capacity. The system in Figure 1 has other advantages such as short random access time (a few microseconds if an

acousto-optic deflector is used) and fast read-out rate (more than 1 gigabit per second is possible with sufficient laser power). In this paper, we do not address these aspects. We will concentrate instead on methods for extending the storage capacity of the basic holographic memory of Figure 1. The method we employ is spatial multiplexing. A recording material with large volume is used and holograms are stored at multiple locations in the material. An additional scanning mechanism is used that allows the recording and read-out beams to access different locations of the holographic medium. The storage capacity of a memory that utilizes spatial multiplexing increases linearly with the number of locations. There are several ways to accomplish spatial multiplexing^{2,11,12}, each distinguished from the others by the scanning method used to address multiple locations. In this paper, we discuss the holographic 3-D disk which employs mechanical scanning mechanism.

II. Holographic 3-D disk

The schematic diagram of a holographic 3-D disk is shown in Figure 2. It consists of a holographic disk (a thick recording material in the shape of a disk mounted on a suitable substrate), a mechanical drive that spins the disk, and a read/write head. The optical head consists of a SLM, relay optics, a mechanism for multiplexing holograms, and a CCD for hologram read-out. The head is essentially a replica of the basic arrangement in Figure 1, and the entire head can translate in the radial direction. Holograms stored at a particular location are retrieved by illuminating the location with a reference beam at the proper angle. The holographic medium can be either a photorefractive crystal, such as LiNbO₃, or a photopolymer film, such as the HRF-150 material that is available from Dupont^{13,14}. In the

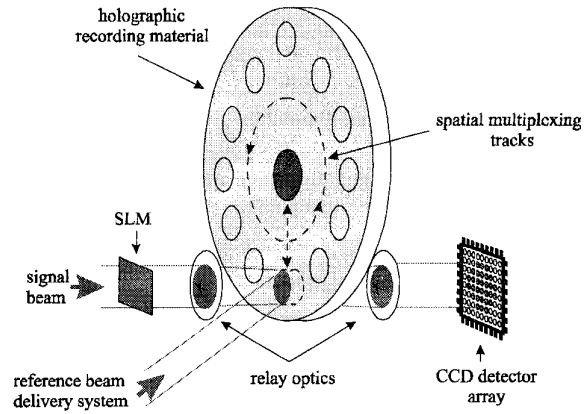


Figure 2 : Holographic 3-D disk setup.

III. Surface Density

The surface density of conventional optical memories (approximately 1 bit/ μm^2) is determined primarily by the size of the illuminating spot. The density of optical CDs will likely increase by an order of magnitude by the end of the decade through the use of shorter wavelength lasers, super-resolution methods¹⁵, and 3-D stacks of recording media¹⁶. To make holographic technology competitive, the density of holographic disks must be higher than the projected density of conventional media by a comfortable margin. To a first approximation, the density of a holographic disk is given by :

$$D_{3D} = M \times D_{2D} \quad (2)$$

where D_{3D} and D_{2D} are the surface densities achievable with a 3-D and 2-D medium, respectively. The maximum number

	Current System	Optimized System
Surface Density	10 bits/ μm^2	40 bits/ μm^2
Medium Thickness	100 μm	100 μm
Number of Holograms	32	32
Recording Rate	.7 Mbits/s (@2 mW/cm ²)	50 Mbits/s (@128 mW/cm ²)
Random Access Time	17 ms (@3600 RPM)	17 ms (@3600 RPM)
Diffraction Eff./Hologram	3×10^{-3}	$\sim 10^{-3}$
Read-Out Rate	.13 Mbits/s (video rate)	> .5 Gbits/s (1000 frames/s)
Estimated Bit-Error-Rate	10^{-4}	?

Table 1: Performance characteristics of the current and optimized system.

remainder of the paper we will describe a specific design of an optical disk system based on the Dupont polymer. The specifications of this system are shown in the first column of Table 1. This particular design does not necessarily have the best specifications possible. These are the specifications that have been demonstrated in our laboratory so far. An estimate of the performance that is possible with a fully optimized 3-D disk using the same recording material is shown in the second column.

of holograms, M , that can be angularly multiplexed at each location is given by :

$$M = \frac{\Theta}{\Delta\theta} = \frac{\Theta L \sin(\theta_r + \theta_s)}{\lambda \cos(\theta_s)} \quad (3)$$

Where Θ is the range of angles that can pass through the aperture of the optical system in the reference arm, $\Delta\theta$ is the angular selectivity, L is the thickness of the hologram, λ is the wavelength of the laser, θ_r , (θ_s) is the angle between

the reference (signal) beam and the disk surface normal. For instance, if we wish to have $M = 100$, we can select $L \sim 300 \mu\text{m}$ assuming $\lambda = 500 \text{ nm}$, $\theta_r = \theta_s = 30^\circ$, and $\Theta = 10^\circ$. We can increase M and hence the density by simply increasing L .

The density predicted by Equation (2) is a theoretical upper limit that can be difficult to achieve in practice. For example, Equation (2) holds only if the resolution of the conventional CD lens and the lens in the signal arm of the system in Figure 2 are the same. This is possible but difficult since the 3-D memory must maintain the same resolution over a large field whereas the CD only needs to produce a single spot at the optical axis of the lens. The recording medium's dynamic range can also limit the storage density since the diffraction efficiency falls off as $1/M^2$. Finally, some noise sources such as cross-talk increase as M gets larger. In a practical system, the storage density is maximized by optimizing the optical design while monitoring the signal-to-noise ratio of the reconstructed holograms.

We have experimentally demonstrated storage density of $10 \text{ bits}/\mu\text{m}^2$ in a $100 \mu\text{m}$ thick Dupont photopolymer film. A diagram of the experimental setup is shown in Figure 3. A glass mask plate of a random binary bit pattern was used as the input SLM. The center-to-center spacing of the pixels was 45 microns and the fill factor was 100%. Nikon F/# 1.4, 3.9 cm aperture camera lenses were used for imaging. A total of 590,000 pixels fit in the apertures of the two Nikon lenses and a sharp image of the entire field was obtained at the CCD plane. The holograms were recorded with a plane reference beam approximately .5 mm past the Fourier transform plane. At that position, the diameter of the signal beam was 1.5 mm and its spatial uniformity was much better than at the exact Fourier plane. The diffraction efficiency as a function of the incident angle of the reference beam is a sinc function¹⁷ centered at the angle at which the hologram was recorded. For the 100 micron thick recording medium, the angular separation to the first null of the sinc function was approximately $.7^\circ$ in our setup. In order to minimize cross-talk between holograms, we angularly multiplexed 8 holograms, each separated by 2.5 degrees. Angle multiplexing was achieved by rotating the film instead of changing the reference beam angle. To increase the density further, we combined angle multiplexing with peristrophic multiplexing⁶. Specifically, sets of 8 angularly multiplexed holograms were recorded at 4 different peristrophic positions. Each peristrophic position corresponds to a different rotational angle of the recording medium around the axis perpendicular to the surface of the medium. Using this method, we stored a total of 32 holograms at a single location. One of the 32 reconstructions is shown in Figure 4. The surface density of each hologram is $590,000 \text{ bits} / (\pi \times .75 \times .75 \text{ mm}^2)$ which is equal to $.334 \text{ bits per micron squared}$. Since 32 holograms are superimposed in the same region, the overall surface density is $32 \times .334 = 10.68 \text{ bits}/\mu\text{m}^2$. In Table 1, we listed $10 \text{ bits}/\mu\text{m}^2$ as the surface density currently demonstrated and $40 \text{ bits}/\mu\text{m}^2$ for the optimized system (both with 100

micron thick medium). We can improve the density of the current system by using lower F/# lenses (higher resolution and density per page), reducing the angular separation between holograms, and increase the range of angles over which holograms can be recorded. The density can of course be increased by a large factor if a thicker recording medium is used.

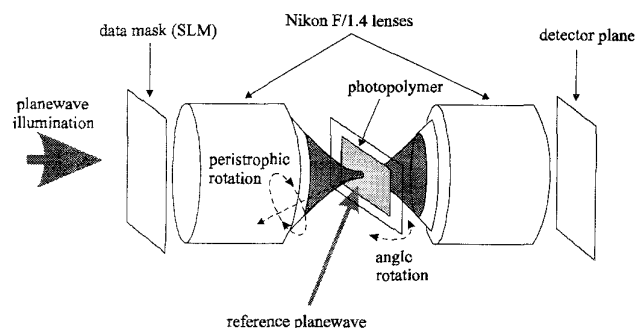


Figure 3 : High density holographic storage setup.

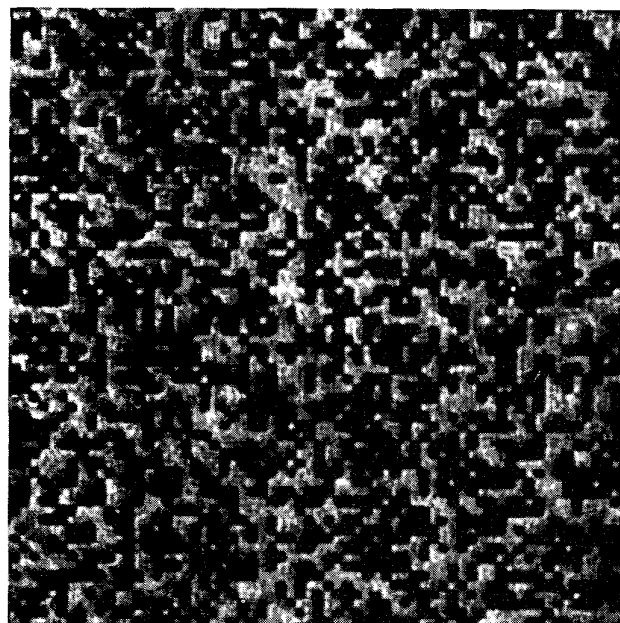


Figure 4 : The reconstruction of one of the 32 holograms stored for the high density experiment.

IV. Recording Rate

The rate at which data can be recorded on the holographic disk is :

$$R_{in} = \frac{N_p}{\tau_{in}} \quad (4)$$

where N_p is the number of pixels per page and τ_{in} is the time required to record one hologram. N_p is primarily limited by the number of pixels on the SLM or the CCD, but it can also be limited in practice by lens aberrations and holographic cross-talk. In our high density experiment, we had 590,000

pixels per hologram. The recording time, τ_{in} , is determined by the sensitivity of the recording medium and the desired diffraction efficiency per hologram. For Dupont's HRF-150 100 micron thick photopolymer, the diffraction efficiency as a function of exposure energy is shown in Figure 5a. The material requires a sensitizing pre-exposure of 35 mJ/cm^2 and the saturation exposure energy is approximately 325 mJ/cm^2 . Notice that Figure 5a is quasi-linear at first but then flattens out as the material nears saturation. This means that the holograms recorded later in the sequence will require a longer exposure time to achieve the same diffraction efficiency as the earlier holograms. An exposure schedule can be derived from Figure 5a so that the diffraction efficiency of the holograms will be equalized. The exposure schedule to deplete all of the material's dynamic range with 50 holograms is shown in Figure 5b and the resulting diffraction efficiency is shown in Figure 5c. Of course, the exposure time per hologram could be considerably shortened if higher intensities were used during recording, or if lower diffraction efficiency holograms can be tolerated. For example, a recording rate of .7 Mbits/s was achieved with our high density experiment (Table 1). This was done by recording 590,000 pixels holograms in an average recording time of 840 ms per hologram. The total incident intensity was 2 mW/cm^2 and the diffraction efficiency per hologram was .35%. From our experimental observations with plane wave holograms, the recording time for achieving the same diffraction efficiency is approximately inversely proportional to the incident intensity for intensities greater than 2 mW/cm^2 . Therefore, if the total incident intensity is increased from 2 mW/cm^2 to 128 mW/cm^2 , then the recording time per hologram drops to 12 ms and the recording rate becomes 50 Mbits/s.

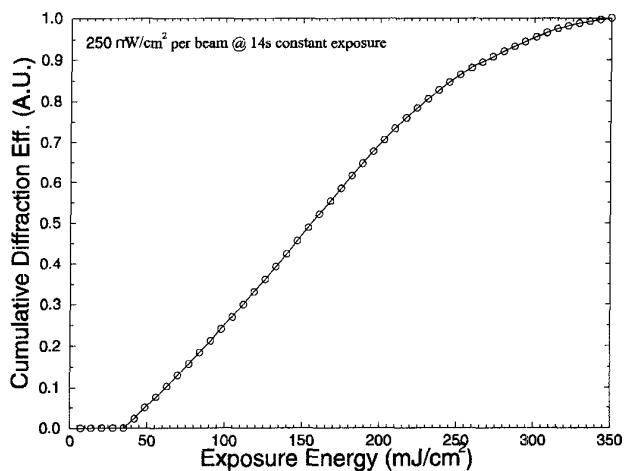


Figure 5a : Diffraction efficiency as a function of exposure energy for the HRF-150-100 photopolymer.

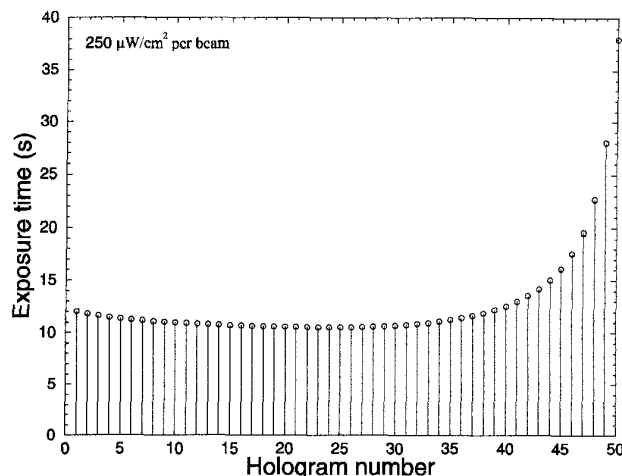


Figure 5b : The exposure time required for each of the 50 holograms in order to equalize their diffraction efficiency.

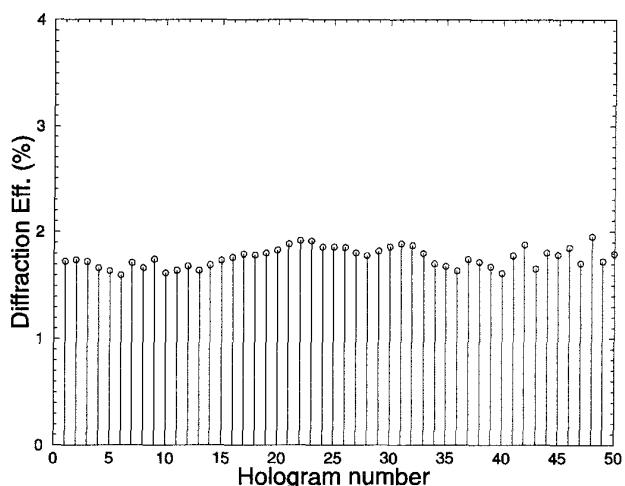


Figure 5c : The resulting diffraction efficiency as a function of hologram number.

V. Read-out Rate

The random access time to any one location is determined by the speed of the mechanical motors that turn the disk and translate the head in the radial direction. For example, if the disk rotates at 3600 RPM, then we can have random access to any angular position on the disk within at most 17 ms. The situation is more complex in a holographic disk since we must properly select the dwell time at each location in order to avoid smearing and to collect a sufficient number of photons for read-out. If the required dwell time is longer than what is afforded by a continuously spinning disk at the maximum speed, then the rotational speed of the motor must be slowed down. The theoretical dwell time required to avoid smearing for an optimum configuration has been computed to be only $2.7 \mu\text{s}$ ¹⁸. Furthermore, if the time it takes to accumulate P photons per pixel is τ , then τ can be expressed as :

$$\tau = \frac{PhcN_p}{\eta I_{inc} \lambda} \quad (5)$$

where h is the Planck's constant, c is the speed of light, N_p is the number of pixels, η is the diffraction efficiency, I_{inc} is the incident power of the reference beam, and λ is the wavelength. For the Dupont HRF-150-100 photopolymer, we experimentally measured the $M/\#$ to be around 6.5, as shown in Figure 6. Therefore, according to Equation 1, the diffraction efficiency per hologram should be about 4% when 32 holograms are multiplexed. For a signal-to-detector noise-ratio of greater than 40:1 with the CCD detector arrays used in our experiment, it is necessary to collect approximately 1,000 photons per pixel. If we chose $N_p = 590,000$, $\eta = 4 \times 10^{-2}$, $I_{inc} = 128$ mW, and $\lambda = 500$ nm, then the required integration time per pixel, τ , is equal to ~ 50 ns. Therefore, the rotational speed of the motors in this case can even be sped up without significant degradation in read-out SNR.

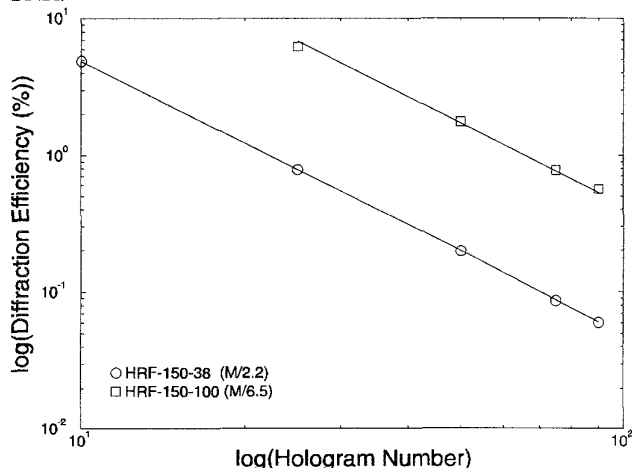


Figure 6 : Diffraction eff. as a function of number of holograms stored ($M/\#$ measurements). The curve with the circles is for a 38 μ m thick film, whereas the squares is for the 100 μ m film used in our experiment.

The expression for the read-out rate, R_{out} , can be simply stated as :

$$R_{out} = \frac{N_p}{\tau_{out}} \quad (6)$$

where N_p is the number of pixels per hologram and τ_{out} is the time required to read each hologram. A read-out rate of .13 Mbits/s was demonstrated in our high density experiment setup (Table 1). Since the reconstructed hologram was much larger than the CCD detector array used, windows of 65×65 pixels from the reconstructed hologram were read-out at video rate with the CCD camera. In the optimized system with full parallelism, a large CCD detector array would be used to read out the entire 590,000 pixels in a minimum frame-transfer-rate of 1000 frames/s to achieve a read-out rate greater than 500 Mbits/s.

VI. Signal-to-Noise-Ratio

Holographic 3-D disks are subjected to many sources of noise such as cross-talk between holograms, lens aberrations, recording material scattering, multiple reflections, noise from the SLM, laser noise, recording material surface imperfections, dust, and the index modulation from previous holograms. There is also the shrinkage effect that is inherent in the photopolymer material, which makes it difficult to Bragg match the entire hologram for read-out. We have studied in detail many of these sources of noise and we minimized them with a proper setup. For our system, we sampled 9 different 65×65 pixel windows from the stored holograms and no errors were detected. The combined histogram from the 9 different sampled windows is shown in Figure 7. It is likely that there were no errors in any of the 32 stored holograms even though we did not check all the stored bits. An estimate for the probability of error was obtained by fitting a first-order χ^2 distribution to the histogram of Figure 7. The estimated probability of error from this model is approximately 10^{-4} . For the optimized system, we do not yet know what estimated probability of error is possible or required for a practical system.

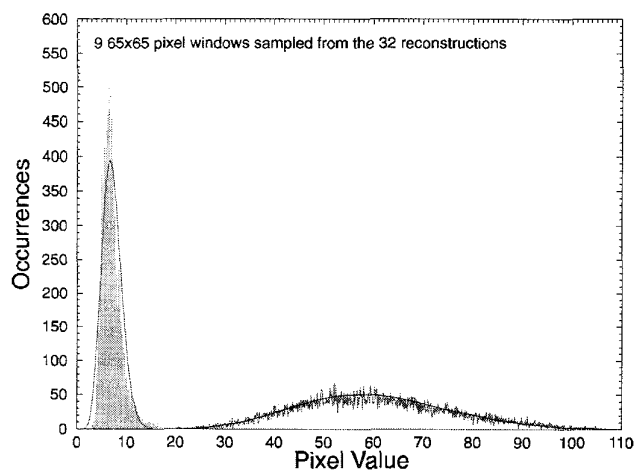


Figure 7 : Combined histogram of the 32 reconstructions.

VII. Acknowledgment

We gratefully acknowledge ARPA for sponsoring this research project.

References

- (1) J. J. Amodei and D. L. Staebler, Appl. Phys. Lett. **18**, pg 540 (1971).
- (2) J. P. Huignard, F. Micheron, and E. Spitz, "Optical Systems and Photosensitive Material for Information Storage," in Optical Properties of Solids, B. O. Seraphin, editor, Chapter 16, pg 847-925, North Holland, Amsterdam, 1976.
- (3) F. H. Mok, Opt. Lett. **18**(11), pg 915 (1993).

- (4) G. W. Burr, F. H. Mok, and D. Psaltis, "Storage of 10,000 holograms in LiNbO₃," *CLEO 1994 Technical Digest*, paper CMB7, pg 9 (1994).
- (5) L. Hesselink, J. F. Heanue, M. C. Bashaw, "Volume holographic storage and retrieval of digital information," OSA Salt Lake City, paper OWA1 (1995).
- (6) K. Curtis, A. Pu, and D. Psaltis, *Opt. Lett.* **19**(13) pg 993-994 (1994).
- (7) D. Psaltis, "Parallel optical memories," *Byte*, **17**(9), pg 179-182 (1992).
- (8) S. Li and D. Psaltis, *Appl. Opt.* **33**(17), pg 3764-3774 (1994).
- (9) D. Psaltis, D. Brady, K. Wagner, *Appl. Opt.* **27**(9) pg 1752-1759 (1988).
- (10) G. W. Burr, F. H. Mok, and D. Psaltis, "Spatially-multiplexed holographic memory optimized for Fourier plane storage in the 90 degree geometry," OSA Annual Meeting, paper MD4 (1994)
- (11) S. Tao, D. R. Selviah, J. E. Midwinter, *Opt. Lett.* **18**(11), pg 912-914 (1993).
- (12) D. Psaltis, M. Levene, A. Pu, G. Barbastathis, and K. Curtis, "Holographic storage using shift multiplexing," *Opt. Lett.* **20**(7), pg 782-784 (1995).
- (13) W. K. Smothers, T. J. Trout, A. M. Weber, and D. J. Mickish, *2nd Int. Conf. on Holographic Systems*, Bath, UK (1989).
- (14) K. Curtis, and D. Psaltis, *Appl. Opt.* **31**, pg 7425 (1992).
- (15) S. M. Mansfield and G. S. Kino, *Appl. Phys. Lett.* **57**(24), pg 2615 (1990).
- (16) K. A. Rubin, H. J. Rosen, W.W. Tang, W. Imano, T. C. Strand, "Multilevel volumetric optical storage," *SPIE Proc. on Optical Data Storage*, Vol. 2338 (1994).
- (17) H. Kogelnik, "Coupled wave theory for thick hologram gratings," *Bell Sys. Tech. J.* **48**, pg 2909 (1969).
- (18) H. Y. Li, "Photorefractive 3-D disks for optical data storage and artificial neural networks," Ph.D. dissertation (California Institute of Technology, Pasadena, Calif.,